

Contents lists available at ScienceDirect

# Cement and Concrete Composites

journal homepage: www.elsevier.com/locate/cemconcomp



# Research Paper

# Rheology of fresh cement pastes modified with nanoclay-coated cements



AlaEddin Douba, Siwei Ma, Shiho Kawashima \*

Columbia University, Department of Civil Engineering and Engineering Mechanics, 500 West 120th Street, New York, NY, 10027, USA

#### ARTICLE INFO

Keywords:
Nanoclay
Cement
Rheology
3D concrete printing (3DCP)
Static yield stress
Nanomaterials dispersion

#### ABSTRACT

Nanoclays (NC) can serve as thixotropy modifiers for fresh concretes, and show potential to meet the rheological demands of 3D concrete printing. Here, we propose a dry dispersion technique that produces NC-coated cement and compare to conventional methods of dispersion. Pastes incorporating NC were tested via shear rheology, scanning electron microscopy, and isothermal calorimetry. Dry dispersion was found to be the most effective method, where incorporating 4.0 wt% NC increased the static yield stress and storage modulus of cement paste by 1500% and 550%, respectively, with a minimal increase in viscosity of 90%. Results of small amplitude oscillatory shear and isothermal calorimetry indicated NC can enhance fresh-state stiffening through seeding, although shear rheology results of kerosene-based cement systems indicated the increase in static yield stress by NC is mainly due to ionic forces. Finally, we discuss how these properties translate to high buildability and stable layer deposition.

# 1. Introduction

Fresh concrete is a non-Newtonian fluid material with rheological properties that vary vastly with respect to chemical composition, particle gradation, environmental conditions, method of preparation and shear history. The interest in 3D concrete printing (3DCP) has generated significant demand for increased understanding of cement rheology and the role of admixtures. Roussel recently identified several rheological properties to be critical for 3DCP, namely static yield stress, dynamic yield stress, critical strain, viscosity, elastic modulus and structuration rate [1]. These rheological properties can be described by colloidal forces driven by Van der Waals attraction and electrostatic forces from adsorbed ions, and progression of cement hydration (e.g. calcium silicate hydrate (C-S-H) bridging) that originate in colloidal flocculation with characteristic time of few seconds [2-4]. The main intrinsic rheological properties resisting failure in 3DCP are static yield stress and structuration rate, as shown in Eq. (1) [1], for systems that do not rely solely on accelerated hardening:

$$\tau_c(t) = \tau_{c0} + A_{thix}t > \rho gH / \sqrt{3}$$
 (1)

where  $\tau_c(t)$  is static yield stress at time t after deposition,  $\tau_{c0}$  is the static yield stress just after deposition,  $A_{thix}$  is the structuration rate,  $\rho$  is the density, g is gravitational acceleration, and H is the total object height. Some more recent works indicated that this equation gives a rather

conservative estimation of the desirable static yield stress for the total object height [5,6]. Of course, other properties such as critical strain, elastic shear modulus and Young's modulus control other factors limiting layer width, height and velocity [1]. Static yield stress, structuration rate, critical strain, and elastic modulus can be further used to describe shape stability – the ability to maintain the deposited layer's shape within tolerable deformation.

In order to meet the high rheological demand of 3DCP, four approaches can be adopted. The first approach is to utilize a number of supplementary cementitious materials (SCMs), such as silica fume (SF) [7–14], fly ash or volcanic ash [9,11–13,15], or ground granulated blast furnace slag (GGBS) [11,12,14,15]. The second approach is to rely on retarder/accelerator systems in which wet concrete supports only a few layers before it completely hardens [9,16-18]. The third approach is to rely on chemical admixtures such as polycarboxylates (PCE) and high-range water reducing admixtures (HWRWA) [8,9,14], or nanomaterials such as purified alumino magnesium silicates (nanoclays (NC) or attapulgite clay) [7-9,11,14,15,19], nanosilica (NS) [10,14] or nanobentonite [ 10, 13]. Of course, these approaches are not mutually exclusive and can be used simultaneously. The variation in cement additives and replacements combined with the scarcity of concrete 3D printers and lack of standards introduce large variations, creating challenges in fully characterizing their effect on printing performance. Furthermore, because cement rheology is shear history dependent, the vast configurations of extrusion and pumping systems in printers can

E-mail address: s-kawashima@columbia.edu (S. Kawashima).

<sup>\*</sup> Corresponding author.

cause additional variations in printing performance.

One of the main challenges faced in 3DCP additives is the coupling effect between rheological properties. For example, an increase in static yield stress and structuration rate is often coupled with an increase in viscosity, potentially compromising pumpability [20]. NC offers great potential for increasing static yield stress and rate of structuration [21-23] with minimal effects on viscosity [8,24,25], also described as exhibiting enhanced thixotropy, and have been shown extensively to improve the printing performance of cement-based composites in terms of buildability [9,11,14,15,19], shape stability [7,8,15], robustness (low variability in static yield stress) [7] and stiffness [19]. Highly purified NC are negatively charged uniformly along their length with high positive charges at their ends that produce a house of card effect in idle solutions [14,24]. It is hypothesized that a similar mechanism is active within the pore solution in NC-cement composites that causes the increase in static yield stress [14,24]. While such claims have not been verified, they will induce strong ionic interactions nonetheless.

As a nanomaterial, the effectiveness of NC is highly dependent on dosage and method of dispersion. Typical contents used in literature are in the range of 0.01-0.5 wt% [7-9,15,19,26,27] while some authors used up to 1.0 [28], 1.2 [11], 2 [14,25], 2.5 [24] and 3 [29] wt.% [11, 14,15], showed that NC has no significant effect on viscosity while [8, 24,25] showed an increase in viscosity. Such discrepancies can be partially explained through differences in preshear conditions [23]. However, they are also a result of the variation in NC dispersion. For example, blending NC in water is the most common way of preparing NC-cement composites [8,9,14,15,19,24,27] while others blend NC dry with cement [7,28,29]. The blending time ranges from 1 to 5 min [15, 24,27] or is unreported [8,9,14,19]. The speed of blending also varies between 140 rpm (1 min) [24], 400 rpm (5 min) [9], and 12 000 rpm (2 min) [27]. Thus, the level of dispersion of NC can be a key reason behind discrepancies in literature. It should be noted that NC also comes in colloidal/liquid pre-dispersed form [30].

Quanji et al. studied the effect of NC dosage and showed that higher contents of NC result in higher static yield stress and degree of thixotropy up to 3.0 wt% [29], but that increasing the dosage of NC beyond 1.3 wt% resulted in a decreased rate of thixotropy. However, dispersion was not the focus of this work and their method of dry mixing NC with cement does not guarantee optimum dispersion. Parveen et al. reported that typical mixing processes employed for mixing in cementitious mortars are insufficient in producing uniform dispersion of nanomaterials such as CNTs [31]. On the other hand, sonication horns/probes are typically classified as the most effective method in deagglomerating and producing uniform dispersion of nanomaterials [32]. However, even when NC are well dispersed in water, achieving a state of uniform dispersion in solution does not guarantee uniform dispersion in the composite [31]. In fact, Yazdanbakhsh and Grasley showed through simulations that achieving uniform dispersion in cement composites requires homogeneous and deagglomerated cement particles [10], which cannot be achieved by adding NC solutions to cement gradually. In order to meet the high rheological demands of 3DCP, high dosage and high efficiency utilization of NC is desired.

In this paper, we implement a dry dispersion method to coat cement grains with NC, producing nanomodified cement. Although this method has been implemented for carbon-based nanomaterials in ceramics [33] and cements [34–37], to the knowledge of the authors it has not been implemented for nanoclays or other inorganic particles in cements. The influence of NC prepared via dry dispersion are compared with that prepared via other methods, i.e. dry mixing and magnetic stirring in solution. NC are incorporated into cement pastes and the pastes are tested for rheological properties, i.e. static yield stress, storage modulus, storage modulus evolution and viscosity, heat of hydration via isothermal calorimetry and scanning electron microscopy (SEM) imaging. We also examine kerosene-based NC cement systems to distinguish Van der Waals from ionic and electrostatic forces. Through the obtained results, we aim to expand upon Roussel's work on the origin of

thixotropy to account for NC interactions, and break down the working mechanisms of NC in cement pastes. Finally, we discuss how the attained rheological properties with NC translate to high buildability potential and stable layer deposition with slenderness ratios of up to 10 for 3D concrete printing.

#### 2. Motivation and background

To fully characterize the kinetics of NC influence on cement rheology, we have used the characteristic soft and rigid interaction mechanisms described by Roussel et al. [2] and expanded it to include the effects of NC by introducing NC-cement and NC-NC interactions. In this work, we refer to all early hydration products including early ettringite formations as C-S-H bridge forces for simplicity. The origin and classification of rigid interactions warrants significant more in-depth analysis of the internal structure, which is beyond the scope of this work but subject of future research. Our analysis of the origin of thixotropy of NC-cement paste is depicted in Fig. 1. The static yield stress is sensitive to all soft and rigid interactions, whereas calorimetry and storage modulus measurements are sensitive only to rigid interactions that govern hydration kinetics. Rigid interactions include nucleation, which is surface-based C-S-H precipitation, and rigidification, which is C-S-H growth. We utilize storage modulus and its evolution similarly to Ref. [23] to rheologically probe and characterize these two phenomena. Calorimetry provides a second layer of investigation as shifts in termination peak time correlate to surface-based C-S-H nucleation and shifts in heat of hydration at the acceleration period correspond to C-S-H growth [38]. On the other hand, the soft interactions that mainly dominate rheological behavior are Van der Waals and ionic forces. To separate NCs effect on the different soft interactions, we study cement systems in kerosene where rigid C-S-H forces are eliminated due to the absence of hydration. Because kerosene is a non-polar solvent, soft colloidal ionic adsorption and electrostatic forces are minimal whereas Van der Waals forces remain unaffected. By comparing NC efficiency in static yield stress and storage modulus, the contribution of soft colloidal forces and rigid interactions can be estimated.

Addition of NC into cement leads to three types of interactions: cement-cement, cement-NC and NC-NC, represented in 2D simplified schematics in Fig. 2 (a), (b) and (c), respectively. According to Flatt's analysis of the measurements of Sakai and Daimon [39], only particles at interparticle distances less than 15-30 nm significantly influence and control cement rheology [3,39]. Because NC's smallest dimension is around the limit of 30 nm, if a cement particle interacts with NC within that linear distance, its interaction with another cement particle within the same linear distance is insignificant to the rheological response. In other words, if an NC needle is sandwiched between two cement particles (as shown in Fig. 2 (b)), the linear distance between these two cement particles must be greater than the width of NC and exceed the 30 nm limit. Hence, there will only be two NC-cement interactions and no cement-cement interactions. Without loss of generality, we can expand on this concept and safely assume that cement-cement interactions are mutually exclusive from NC-cement interactions. Of course, multiple NC needles can be between cement particles and induce additional NC-NC interactions. Therefore, a cement particle will either interact with another cement particle or NC particle but NC particles can interact with cement and other NC particles simultaneously. The mix of these interactions are visualized in Fig. 2 (d) and (e). Ultimately, cement paste is a complex system that utilize a mix of all such forces within a 3D space as visualized in (f). Nevertheless, such analysis remains a simplified first-order approximation and further rigorous analysis can be used to gain more quantitative interpretation of the system.

To better understand the relationship between cement-NC and cement-cement interactions, we can estimate the percentage of cement particle surface area that can be theoretically covered by well dispersed NC, %A<sub>cover</sub>, measured according to Eq. (2):

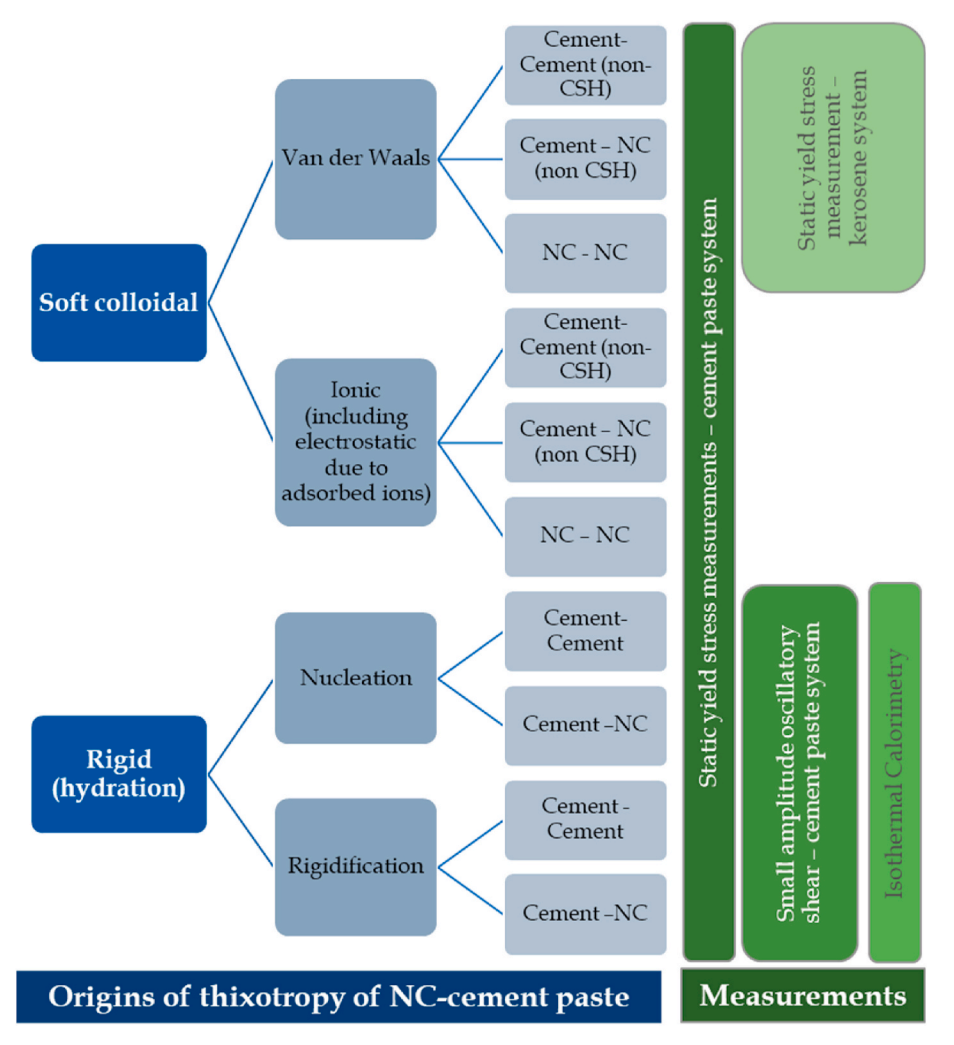


Fig. 1. Evaluation carried of the origin of thixotropy of NC-cement paste with reference to N. Roussel's work [2].

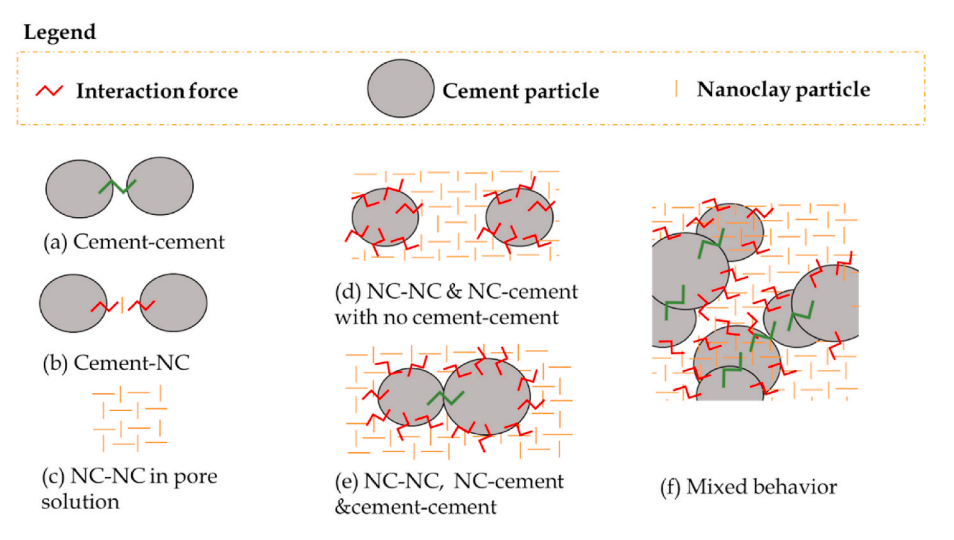


Fig. 2. Simplified 2D-schematics of the interactions that influence cement rheology in NC cement paste system.

$$\%A_{cover} = \frac{Total \ surface \ area \ of \ NC}{Total \ surface \ area \ of \ Cement}$$

$$= \frac{SSA \ of \ NC^*wt.\%^*solid \ density \ of \ NC}{SSA \ of \ cement^* \ (1 - wt.\%)^*solid \ density \ of \ cement}$$
(2)

The specific surface area (SSA) is defined as the surface area per unit

volume. Cement has an SSA around 1  $\rm m^2/g$  [40] while NC similar to the one used in this paper have been measured as 107  $\rm m^2/g$  using BET method [41]. Given that the solid density of NC is 2.287 g/cm<sup>3</sup> [26] and the solid density of cement is 3.15 g/cm<sup>3</sup>, %A<sub>cover</sub> for the different NC dosages used is shown in Table 1. The first limit of %A<sub>cover</sub> represents the

Table 1
Percentage of cement particles surface area that can be covered by NC in well dispersed state.

NC (wt.%)		1%	2%	3%	4%
%A <sub>cover</sub>	First limit	78%	159%	240%	324%
	Second limit	39%	80%	120%	162%

case where NC is sandwiched between two cement particles, while the second limit represents the case where NC covers the surface of cement on one side and is free on the other, effectively reducing the contact SSA by half. While the second limit seems more likely, it also assumes that all NC needles will be densely packed on the surface of the cement. However, because NC needles are negatively charged along their length, such dense packing is energetically unfavorable. Thus, the values of  $\% A_{\rm cover}$  presented aim to provide limits to when all the surface of cement will be covered. In actuality,  $\% A_{\rm cover}$  decreases due to NC and cement agglomeration and increases due to cement dissolution. Therefore, we consider our theoretical limit only at the beginning of dissolution processes and with effective dispersion.

The extreme dimensionality of NC is clearly reflected by the exceptionally high values of  $\%A_{cover}$  exceeding 100% within the tested NC dosage. In fact, within 1.27-2.54 wt%, well dispersed NC have an effective surface area to cover the surface area of cement particles completely. Hence, if all cement particles are covered by NC particles, the interaction between two cement particles is insignificant to cement rheology, as they exceed 30 nm in spacing. This means that increasing the content above 1.27-2.54 wt% in well dispersed states allows only for additional NC-NC interactions where cement-NC are maximized and soft cement-cement interactions are eliminated. However, due to nucleation and seeding effects of NC, some additional rigid cement-cement interactions can still occur. Because cement dissolution and hydration are such complex phenomena and the challenges in measuring the state of NC dispersion within cement paste at a few 10s of seconds after deflocculation, this theoretical model cannot be verified experimentally. However, this discussion highlights some key aspects on the effect of NC addition to soft colloidal cement interactions.

- There is a theoretical limit at which nanomaterials in general can interact with cement. Beyond such limit, the main additional interactions within the system are nanomaterial interactions like NC-NC.
- 2. There is an exchange between soft cement-cement and NC-cement interactions due to the addition of NC given their geometry.
- 3. The state of NC dispersion plays a key role in controlling the mechanisms of NC interactions, as such has a direct influence on their effective SSA and in turn the dosage at which  $\% A_{cover}=100\%$  is achieved.

#### 3. Materials and methods

#### 3.1. Materials

Ordinary Type I cement and distilled water were used to prepare pastes. The chemical composition of the cement is provided in Table 2. Different levels of NC substitution by weight of cement were used in this study ranging from 0.5 to 4.0 wt%. Table 3 summarizes all mixes with NC content based on their dispersion method. The prefix in NC mixes

**Table 2** Chemical composition of cement.

Content (%)						Loss on ignition (LOI)
SiO <sub>2</sub>	$Al_2O_3$	Fe <sub>2</sub> O <sub>3</sub>	CaO	MgO	$SO_3$	
19.27	4.68	3.51	63	3.21	2.72	2.09

**Table 3**Mixes list and reference information.

Information	Mix type	Magnetic stirring (mag)	Dry mix (dm)	Dry dispe	ersion (dd)
	Cement type	Unprocessed cement Water		Cement processed through dry dispersion	
	Solution liquid				Kerosene
	Reference mix	Neat		Neatdd	Neatddkero
NC content (wt.%)		Abbreviation			
0.5		0.5 NCmag	_	-	_
1.0		1 NCmag	1NCdm	1NCdd	1NCdd_kero
1.5		1.5 NCmag	-	-	-
2.0		2 NCmag	2NCdm	2NCdd	2NCdd_kero
2.5		2.5 NCmag	-	-	-
3.0		3 NCmag	3NCdm	3NCdd	3NCdd_kero
4.0		-	4NCdm	4NCdd	4NCdd_kero

represents the content as weight replacement of cement and the suffixes are; "mag" referring to NC dispersed in water via magnetic stirring, "dd" referring to NC dispersed on cement via dry dispersion, and "dm" referring to NC that is added in the dry, as-received state during mixing. Neat refers to the reference paste that is unprocessed and Neatdd is reference cement that undergoes the dry dispersion process without NC presence. Neat, mag, dd and dm mixes were prepared using water-tobinder (w/b) ratio of 0.34 by mass. Additionally, in some mixes the water content was completely replaced with kerosene, a nonpolar solvent (dielectric constant  $\varepsilon = 1.8$ ) with an absolute viscosity of 0.00164 Pa s, as the liquid phase to diminish the influence of electrostatic force between particles and hydration. They are denoted with "\_kero". Kerosene mixes were prepared using similar mass ratio of 0.34. The cementkerosene pastes stayed homogenous and no bleeding was observed during the tests. The negative and positive charges along the length and ends of the NC, respectively, introduce dipole-dipole forces in polar solvents (e.g. water), which allows dispersion without the need to introduce additional chemical forces via surfactants. Because kerosene is non-polar, all kerosene systems used dd cements, as a stably dispersed NC suspension cannot be achieved in kerosene at the studied addition range without introducing additional chemical forces. Because NC are added as replacement of cement, a dilution effect is expected decreasing cement-cement interactions and reducing the maximum heat of hydration similar to increasing the w/b from 0.34 to 0.354 at 4 wt%.

#### 3.2. Mixing

Magnetic stirring (mag) was used to prepare a solution dispersion of NC in distilled water at 400 rpm for a minimum of 1 h. A large solution of 350–400 mL was produced, which was always stirred immediately before use to prepare cement pastes. Dry mixing (dm) cement paste was prepared by using a hand mixer for 15 s to combine cement with NC powder, before adding distilled water. Dry dispersion (dd) is detailed in the following section.

Special care was taken to ensure all pastes had similar shear history leading up to rheological testing. To prepare mag cement paste, the NC solution was added to the cement, whereas in the case of dm or dd paste distilled water was added to the cement and NC composite. This process was done within 30 s and NC, cement and water were then mixed for 120 s at similar speed using a hand mixer. The highest mixable content of NC in solution was 3.0 wt%. The paste was then loaded into the cup and vibrated for 5 s to remove air bubbles before loading into the rheometer. The vane was inserted 600 s from the time of contact between cement and water. A similar mixing approach was used for calorimetry but the paste was added to a glass vial and inserted in the

calorimeter 300-330 s from the time of contact between cement and water.

### 3.3. Dry dispersion

The basics of the approach reported by Refs. [33-37] were further developed to ensure ease of repeatability and applicability to a diverse selection of nanomaterials. Isopropyl alcohol was replaced with ethyl alcohol, magnetic stirring was used in conjunction with probe sonication, distillation was used in place of desiccation or evaporation, and magnetic stirring was used through distillation. NC were first sonicated continuously in ethanol solution at 10 kJ/g NC while being simultaneously stirred using a magnetic stirrer. The energy used in this step is twice the one reported by Ref. [10] since dispersion in ethanol is more challenging than in water due to its lower polarity at relative polarity of 0.654. Ethanol was used instead of other alcohols due to its low boiling temperature and polarity. The solution was kept inside an ice bath to prevent excessive evaporation of the ethanol. Cement was then introduced to the solution maintaining continuous sonication and stirring. Sonication was applied to achieve 30 kJ/g NC after addition of cement at 2 s pulses. The NC-cement ethanol solution was then moved to a distillation apparatus to recover the ethanol. During distillation, the solution was also stirred to minimize sedimentation. 80% of the original ethanol was recovered within 30 min. The NC coated cement cake was then broken down and placed in a drying oven set at 260 °F (126 °C) for 24-48 h to ensure complete removal of ethanol and to prevent hydration with air moisture. Upon removal of cement, the cement grains were further processed using mortar and pestle and kept in airtight bags until mixing with water to produce NC-cement pastes.

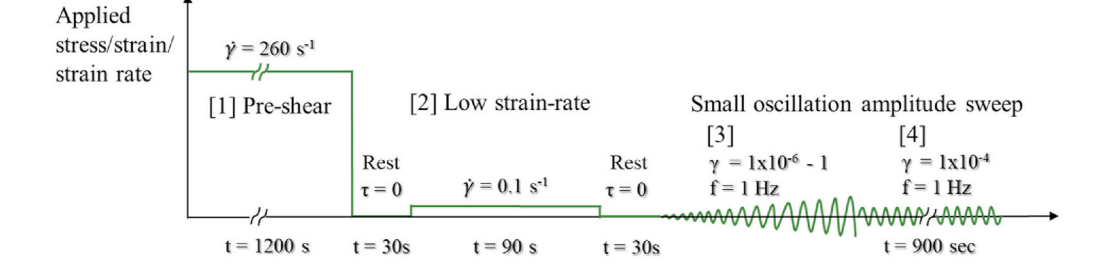
#### 3.4. Rheological protocol

A four-blade vane and cup geometry were used in a stress-controlled HAAKE MARS III rheometer set at 25 °C. The cup had an inner diameter of 26.6 mm, the vane blades were 21.9 mm wide and the gap between the vane and the cup was 8 mm. At least three different measurements were collected per mix, where up to 7 additional tests per mix were carried out when variance was greater than 10%. This ensures that results with means greater than  $1\pm0.074$  times the mean are different at a 95% confidence interval, which was considered to be sufficient in this study when shear history was similar. Five mixes required additional tests – 1 NCmag, 1.5 NCmag, 2 NCmag, 2NCdm and Neatddkero. Shear

history of 3DCP materials depend on the type of reservoir, pump, transportation and extrusion system of the printer. Thus, it is critical for rheological studies to examine the rheological properties of cementbased materials from a reference deflocculated state. High contents of additive that target high structural build up (as demanded by 3D printing processes) require significantly longer preshear to reach a deflocculated steady state [23]. Such is especially critical for NC, which are charged particles that significantly increase the rate of flocculation [27,42,43]. Thus, a relatively long preshear of 20 min was used in this study to ensure all tests were at a well-defined reference state. It should be noted that for NC prepared in solution via magnetic stirring, at high NC contents the cement paste was too stiff and no flow could be initiated by the rheometer, as it exceeded the equipment's maximum torque. Therefore, mixes containing 2.5 and 3.0 wt% (2.5 NCmag and 3.0NC mag) required manual initial torquing to initiate structural breakdown prior to applying pre-shear to protect the testing apparatus.

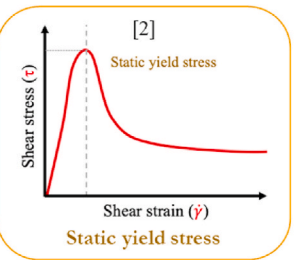
The rheological protocol is described in Fig. 3. It starts with a preshear, where the dynamic viscosity was determined once steady state was reached. The prolonged preshear was needed to ensure all mixes reached a steady state response before measuring the static yield response, as shown in Fig. 4. Following the preshear, a rest period of 30 s using a zero-stress condition was applied to allow for structuration. A strain rate of 0.1 s<sup>-1</sup> was then applied to measure the static yield stress. Another zero-stress rest period was applied for 30 s, then small amplitude oscillation shear (SAOS) was applied at a frequency of 1 Hz and logarithmic strain sweep from  $1 \times 10^{-6}$  to 1 1/s. The storage modulus G' was continuously recorded, where there was an initial linear viscoelastic regime (LVR), where G' is nearly constant, followed by a drop, which marks the end of the LVR and indicates irreversible damage to the rigid structure. The applied strain amplitude corresponding to the end of the LVR is identified as the rigid critical strain, which is typically of the order of a few  $10^{-4}$  [2]. The storage modulus at such strain levels can then be interpreted as the elastic modulus according to linear viscoelasticity principals. Finally, we capture the evolution of the storage modulus over time by applying a strain of  $1 \times 10^{-4}$  at a frequency of 1Hz over 30 min. Analysis of the storage modulus followed the work done by Ma et al. based on Eq. (2), where c is a fully developed structural parameter condition,  $\theta$  is the relaxation time, t is the time parameter and Grigid is the rate of linear evolution of storage modulus [23].

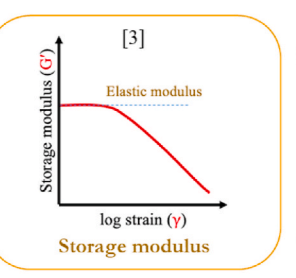




# Response







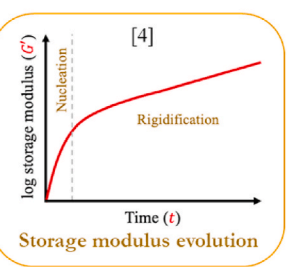


Fig. 3. Rheological protocol (Time is not to scale).

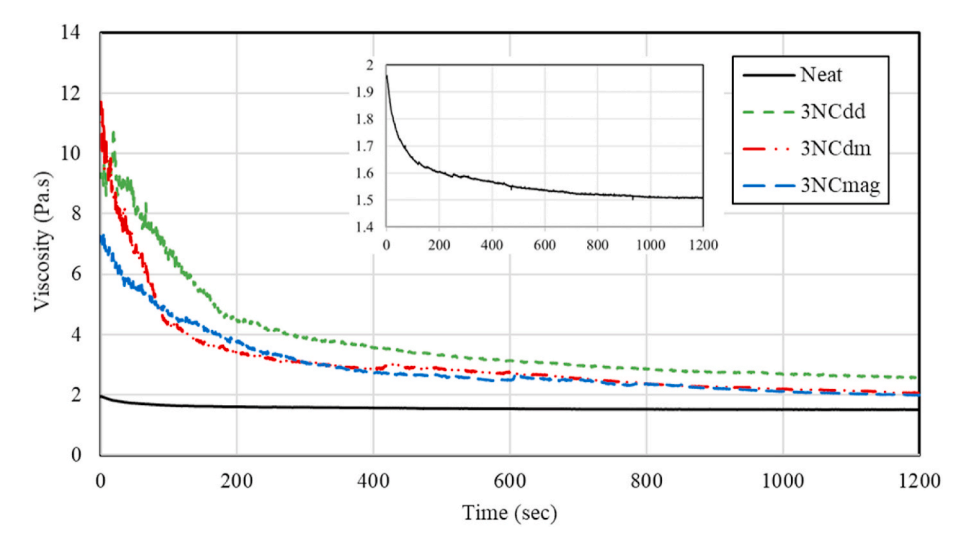


Fig. 4. Viscosity evolution during pre-shear at 3 wt% NC addition dispersed via dry dispersion, dry mixing, and magnetic stirring compared to Neat (enlarged in subfigure).

$$G' = c \left( 1 - e^{-\frac{t}{\theta}} \right) + G_{rigid}t \tag{3}$$

Our protocol measured dynamic viscosity, static yield stress, and storage modulus in series, in order to reduce the overall number of tests and to simulate the 3DCP process. In a general extrusion-based 3D concrete printing scheme, the fresh cement-based material is subjected to prolonged shearing during pumping and extrusion, then deposited, where the deposited layer is able to hold its shape if it exhibits sufficient green strength to sustain self-weight induced stresses and in some cases the weight of subsequent layers. The initial pre-shear simulates shearing from pumping and extrusion, from which we obtain corresponding viscosity. From there, static yield stress is measured to determine the capacity for shape stability shortly after deposition. And finally, the fresh material's stiffness and evolution over time will indicate the extent of elastic deformation of the layer, as well as overall structural stability, as printing continues. So although the static yield stress and storage modulus of a given paste sample will be measured at different shear histories, these parameters can be directly compared against different mix designs, which was the aim of this study.

#### 3.5. Calorimetry

The hydration kinetics were investigated for the hydrating mixes (excluding kerosene system) at 25  $^{\circ}\text{C}$  using isothermal calorimetry (TAM Air III). A new paste was prepared for each test. 5 g of paste was loaded inside each standardized glass ampule, where a total of three tests were performed per mix. Data was collected for 48 h and all samples generated a total of 185 kJ  $\pm$  3 kJ by 36 h indicating the generation of a similar total amount of hydration products.

# 3.6. SEM scans

Scanning electron microscope images were collected for NC powder and unhydrated 2.0NCdd powder, as well as 7-day air-cured 2.0 NCmag and 2.0NCdd cement pastes. 2.0 wt% content was selected as the median content examined in this paper. All samples were coated with 1 nm gold palladium (Au–Pd) via 108 Manual Sputter Coater. Scans were collected using Zeiss Sigma VP SEM with a resolution of 12 Å at 2–5 kV. Hydrated samples were obtained from fractured pieces of hardened cement samples that were produced using the same mixing approach as described prior.

#### 3.7. Particle size analysis

The particle size distribution was measured using Beckman Coulter Laser Diffraction Particle Sizing Analyzer; LS 13 320. The device has a working range of 17 nm–2000  $\mu m$  and uses a sonicated aqueous submersion technique. This test was utilized to examine the effect of dry dispersion processing on the cement particle distribution. Plain cement was processed at similar energy to that used for 1NCdd and the difference in particle distribution before and after was recorded.

# 4. Results

# 4.1. SEM

The extreme dimensions of nanomaterials generate high surface energy as the number of atoms on the surface are higher than those inside, reaching upwards of 50% at 3 nm. As a result, nanomaterials such as NC tend to agglomerate in order to reduce their free surface energy and stabilize [31]. Fig. 5 shows evidence of this phenomenon by looking at NC in the as-received, dry state, where agglomerates are at the micron level (Fig. 5 (a)), while also emphasizing the uniformity and dimensionality of the NC used in this study (Fig. 5 (b) and (c)).

Typical dispersion methods are applied for nanomaterials in water so the dispersive state of NC can only be investigated in solution prior to combining with cement, or post hydration. Imaging post hydration however requires high resolution environmental SEMs and the ability to arrest hydration abruptly and rapidly. For example, Makar and Chan were able to utilize FEG-SEM and flash freezing using liquid nitrogen to examine growth of hydration products and the dispersive state of single walled CNTs [34]. Because dd coats cement with NC in the absence of water (and hydration products, as a result) scans such as the one shown in Fig. 6 can be collected using typical SEM equipment, showing unhydrated cement particles and dry NC. It is apparent that through dd, the cement particles can be effectively coated with singly dispersed NC particles. Furthermore, the geometries of NC observed in Fig. 5 are preserved.

#### 4.2. Effect of dry dispersion

Cement powder was tested before and after dd processes to examine the effect of sonication and distillation on the cement particle gradation and rheology. As a result of dd, particles sized in the 100–200  $\mu m$  range completely disappeared in Neatdd, as shown in Fig. 7. A higher number of finer particles was observed, especially in the 0.3–2.5  $\mu m$  range. This

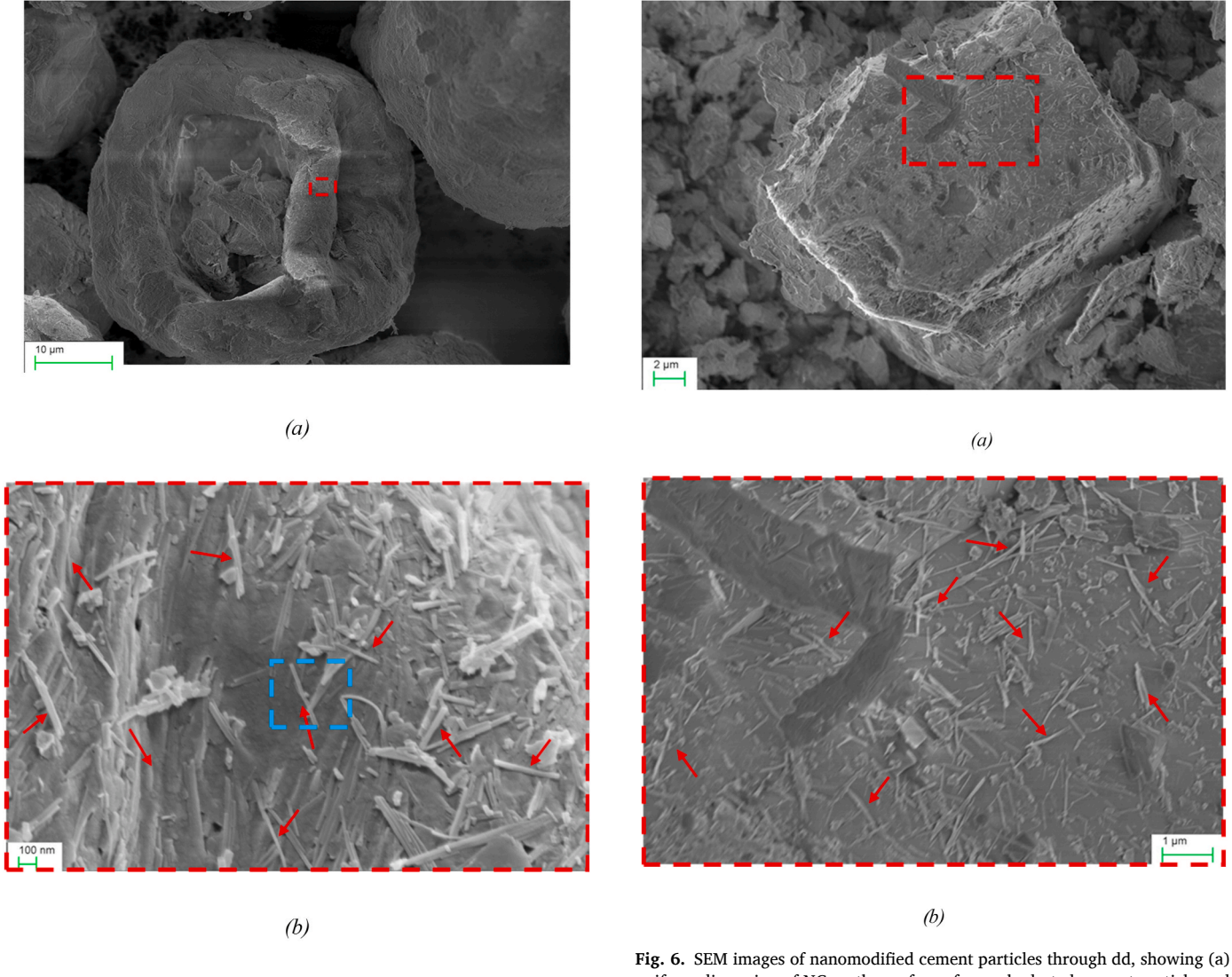


**Fig. 6.** SEM images of nanomodified cement particles through dd, showing (a) uniform dispersion of NC on the surface of an unhydrated cement particle and (a) close-up of individual well-dispersed NC needles.

decrease can be described statistically by an overall 8% decrease in particle size mean and a reduction from 2.26  $\mu m$  to 1.65  $\mu m$  of the particle size threshold occupying 10% by volume. These findings agree with Makar and Chan and are attributed to the high sonication energy applied to the system [31]. Makar and Chan also identified the reduction in particle size to be primarily in the gypsum phase [31]. The rheological properties were also measured and show a decrease in static yield stress of 16% (from 141 Pa to 118 Pa), a decrease in storage modulus of 27% (from 2.9  $\times$  10 $^5$  Pa to 2.1  $\times$  10 $^5$  Pa) and a decrease in viscosity by 8% (from 1.59 Pa s to 1.47 Pa s). Therefore, herein pastes where NC is introduced via mag or dm are compared against Neat, while those where NC is dry dispersed are compared against Neatdd to isolate the effect of NC.

# Pa 1 = 25.48 nm

**Fig. 5.** SEM images of NC dry powders in the "as-received" reference state at increasing magnifications: (a) NC agglomerated to the micron scale; (b) individual NC needles clumped together; (c) measurement of individual NC needle.

#### 4.3. Rheology - NC-cement paste system

The rheological responses of NC-cement pastes at different NC contents were measured for all three dispersion methods. Fig. 8 shows the results of static yield stress normalized by their respective reference pastes Neat and Neatdd, which exhibited static yield stress values of 141 Pa and 118 Pa, respectively. It is worth noting that replacement of cement is associated with reduction in static yield stress due to a decrease in cement-cement interactions due to dilution. However, the

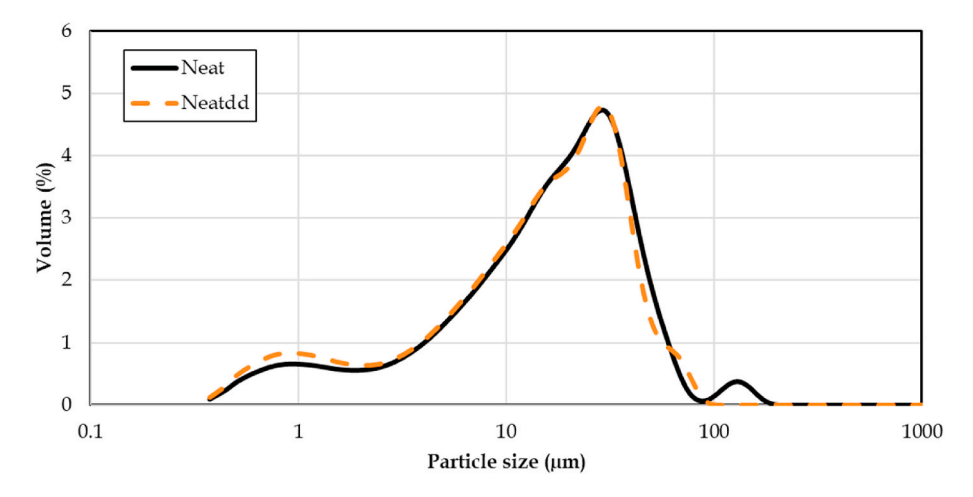
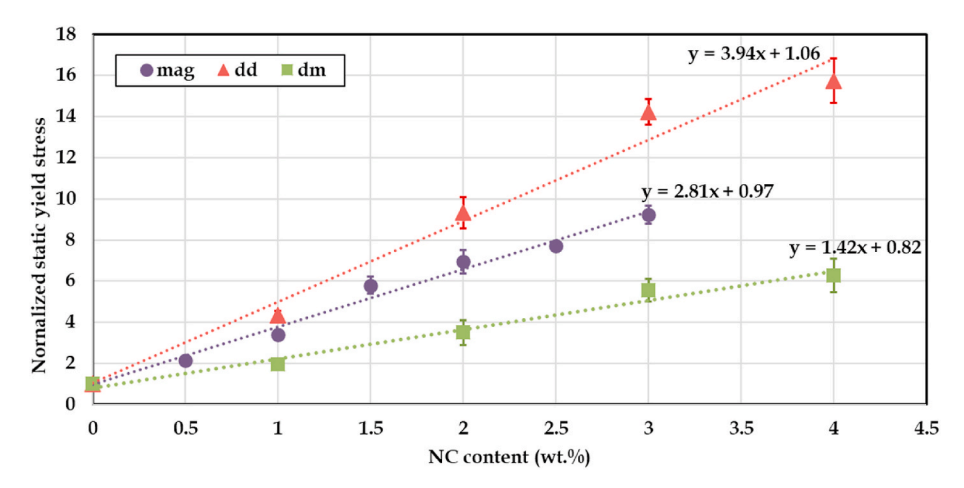


Fig. 7. Particle size analysis results for reference cement before and after dry dispersion processes.



**Fig. 8.** Normalized static yield stress as a function of NC content using different dispersion methods, where the static yield stress is normalized with respect to Neat (141 Pa) for mag and dm and Neatdd (118 Pa) for dd (Linear regression lines with average R<sup>2</sup> value of 0.982).

addition of the new NC-NC and NC-cement interactions mitigate all decrease, and the effects are negligible on the static yield stress. It is evident that NC is successful in increasing static yield stress regardless of dispersion method, and increase in effectiveness increases with

dispersion energy, where the highest is dd followed by mag then dm. Compared to dm, mag and dd show 1.98 and 2.77 times increase, respectively, in the efficiency of NC, which is taken to be the slope of the regression lines. This translates to lower contents of NC to reach a target

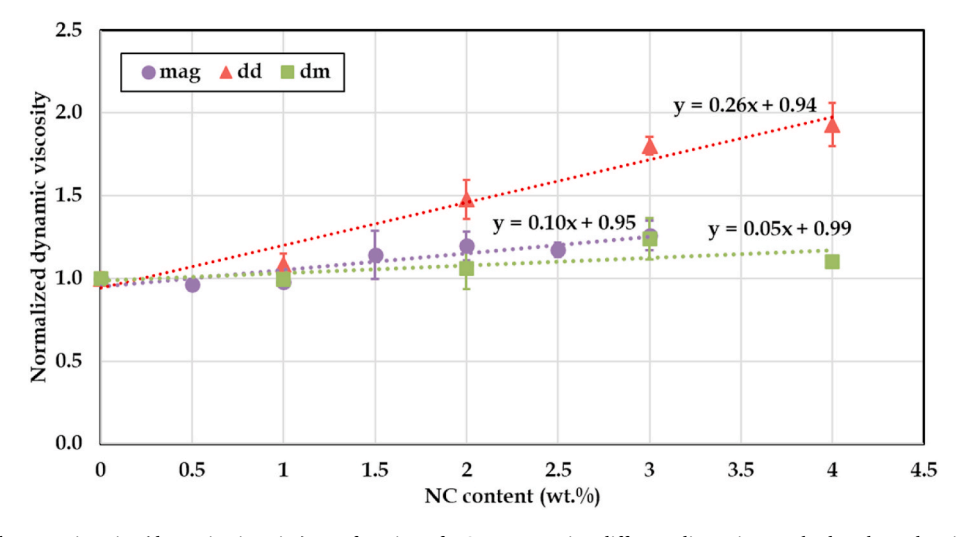


Fig. 9. Normalized steady state viscosity (dynamic viscosity) as a function of NC content using different dispersion methods, where the viscosity is normalized with respect to Neat (1.6 Pa s) for mag and dm and Neatdd (1.5 Pa s) for dd (Linear regression lines with average R<sup>2</sup> value of 0.86).

yield stress, e.g. to achieve the same static yield stress achieved by 1 wt% NC dispersed via dm, only 0.5 and 0.35 wt% NC would be required if dispersed via mag and dd, respectively. Furthermore, up to 4 wt% NC content was incorporated successfully via dd, reaching an increase in static yield stress by around 1500% to 1860 Pa at 0.34 w/b ratio (4NCdd).

The results of dynamic viscosity, which was measured as the steadystate viscosity, is shown in Fig. 9. Reported values are normalized by their respective reference pastes Neat and Neatdd, which exhibited viscosity values of 1.6 Pa-s and 1.5 Pa-s, respectively. The results of mag and dm show statistically insignificant changes in viscosity at NC contents up to 1.5 and 2.0 wt%, respectively, but increases by up to 25% compared with Neat at higher contents irrespective of NC content. Dd showed little change at 1 wt% but an increase in viscosity beyond 1.0 wt %, reaching 90% increase compared with Neatdd at 4.0 wt%. Still, the increase in viscosity is not prohibitively high for 3DCP processes. For example, Zhang et al. tested the buildability of different mixes with viscosities in the range of 3.5-4.5 Pa s and reported excellent fluidity [14] where the highest viscosity reported in this work is that of 4NCdd at 2.8 Pa s. Furthermore, the increase in viscosity is significantly less than the increase in static yield stress, which ranges from 500% to 1500% for 2NCdm and 4NCdd, respectively. Variations in the NC's effect on viscosity due to dispersion method and content can potentially explain the variations observed by different authors on the effect of NC on viscosity, where [11,14,15] showed that NC has no significant effect on viscosity while [8,24,25] showed an increase in viscosity.

Storage modulus measurements from the SAOS amplitude sweep are presented in Fig. 10. In plain cement paste systems, the storage modulus at strain values in the order of few  $10^{-4}$  is associated with C–S–H links [2]. These rigid interactions can be classified as cement-cement or cement-NC for NC modified cement pastes. And an increase in storage modulus can be an indicator of additional C–S–H links, thicker ones or combination of both, and can be used to compare NC addition level and dispersion method. It should be noted that although we will continue to refer to the origin of the rigid structure as C–S–H links/bridges for simplicity, it can be attributed to the formation of any early hydrates.

Storage modulus results show higher degree of sensitivity to dispersion energy compared to static yield stress, where the NC efficiencies are 3.68 and 6.9 times higher for mag and dd, respectively, compared to dm. Such findings suggest that higher dispersion energy could correspond to more uniformly dispersed, single NC needles enhancing degree of percolation and subsequent nucleation and rigidification, or serving as links themselves. It should be noted that this is subject to the limit of energy to achieve uniform dispersion without damaging the particles. The origin of the increase in storage modulus is further examined by looking at the evolution of the storage modulus and

examining the hydration kinetics through calorimetry.

In addition to obtaining G' from the amplitude sweep, we also monitored G' evolution to obtain a measure of rate of stiffening. Applying Eqn (3), we focused our analysis on Grigid, i.e. rate of linear increase of G' over time, which is considered to be a measure of rigidification due to the growth of early hydrates. The results are shown in Fig. 11. Regardless of dispersion method, the addition of NC caused an increase in G<sub>rigid</sub>, indicating an increase in rate of rigidification. Both dm and mag reached their maximum increase in Grigid within 3.0 and 2.0 wt % NC, respectively. The addition of NC beyond these contents showed a decrease in Grigid while maintaining an overall increase compared to Neat. Dd showed an increase in Grigid proportional to NC content up to 2.0 wt%, but at 3.0 and 4.0 wt% there was a significant increase in measurement variation, making the difference statistically insignificant. Therefore there seems to be a threshold level for all dispersion methods, beyond which no increase in Grigid is observed. Additionally, in contrast to previous results on static yield stress and storage modulus, mag had higher NC efficiency for G<sub>rigid</sub> compared to dd up to 2.0 wt%. Although the results of storage modulus captured a steady increase in G' with NC content and dispersion energy, suggesting enhanced nucleation and growth of hydrates, this was not seen in the results of G<sub>rigid</sub>. Considering all these observations, it is clear that the influence of dispersion on structural build-up kinetics is more complex. The role of NC on potential seeding effects and hydration kinetics was explored further via isothermal calorimetry, and will be discussed later on.

According to Roussel et al., there exist rigid and soft colloidal critical strains associated with the breakage of C-S-H links and colloidal network which are at the order of few hundredths % and few % strains, respectively [2]. At the order of few % strain and prior to yield, the stiffness of the percolated network is governed by soft colloidal interactions as rigid C-S-H links are ruptured past the rigid critical strain [2]. Nevertheless, the yield stress is still a function of the stress required for the breakage of both networks. Consequently, the macroscopic stress  $au_{macro}$  (the stress applied to the percolated network up to and within the yield stress) can be expressed as a product of the macroscopic strain  $\gamma_{macro}$  in the order of few % and macroscopic elastic modulus  $G'_{macro}$ ; that is,  $\tau_{macro} = G'_{macro} \gamma_{macro}$  [2]. Hence, we measure  $G'_{macro}$  within the linear regions of the stress-strain response where the strain is in the order of few % representing the stiffness of the soft colloidal network and the results are shown in Fig. 12. Fig. 13 shows the stress-strain response at 3 wt% NC as representatives of each dispersion method in comparison to the reference pastes, Neat and Neatdd, where the dashed lines represent the linear region where  $G'_{macro}$  is measured.

Similar to previous results, high  $G'_{macro}$  sensitivity was observed with dd followed by mag then dm. With respect to each dispersion method on static yield stress, storage modulus and  $G'_{macro}$ , NC efficiency showed

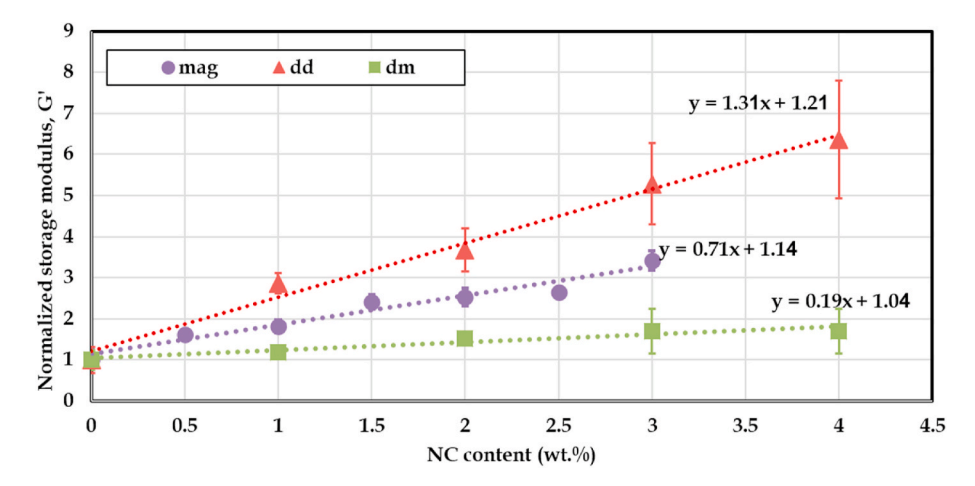


**Fig. 10.** Normalized storage modulus (G') results as a function of NC content, where G' is normalized with respect to Neat ( $2.1 \times 10^5$  Pa) for mag and dm and Neatdd ( $2.1 \times 10^5$  Pa) for dd (Linear regression lines with average R<sup>2</sup> value of 0.953).

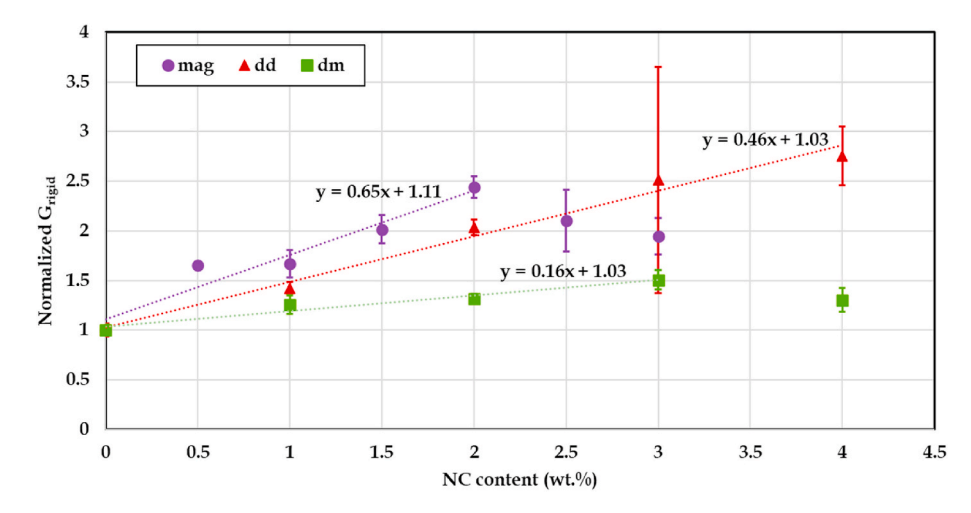


Fig. 11. Normalized rate of linear increase of storage modulus ( $G_{rigid}$ ) as a function of NC content, where  $G_{rigid}$  is normalized with respect to Neat (173.6 Pa/s) for mag and dm and Neatdd (177.0 Pa/s) for dd (Linear regression lines with average  $R^2$  value of 0.89).

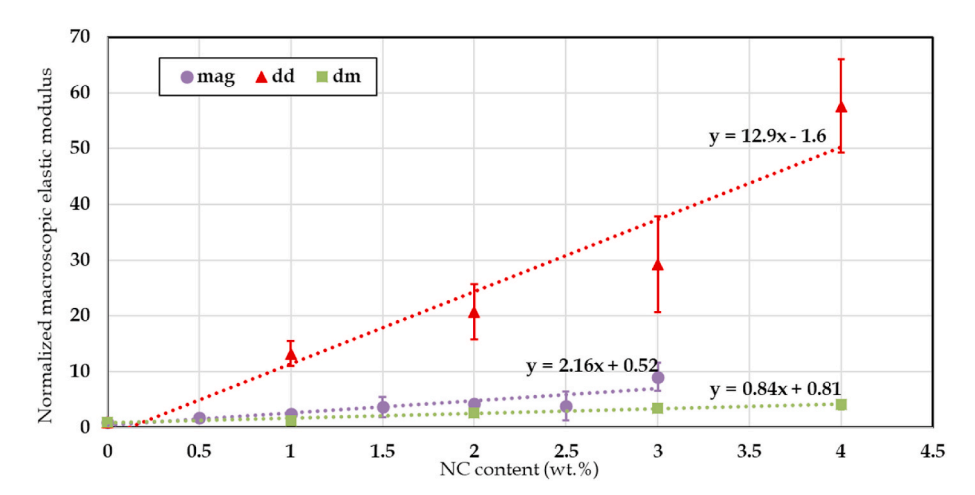


Fig. 12. Normalized macroscopic elastic modulus as a function of NC content, where modulus is normalized with respect to Neat  $(1.9 \times 10^4 \text{ Pa})$  with respect to mag and dm and Neatdd  $(3.6 \times 10^3 \text{ Pa})$  for dd (Linear regression lines with average  $R^2$  value of 0.89).

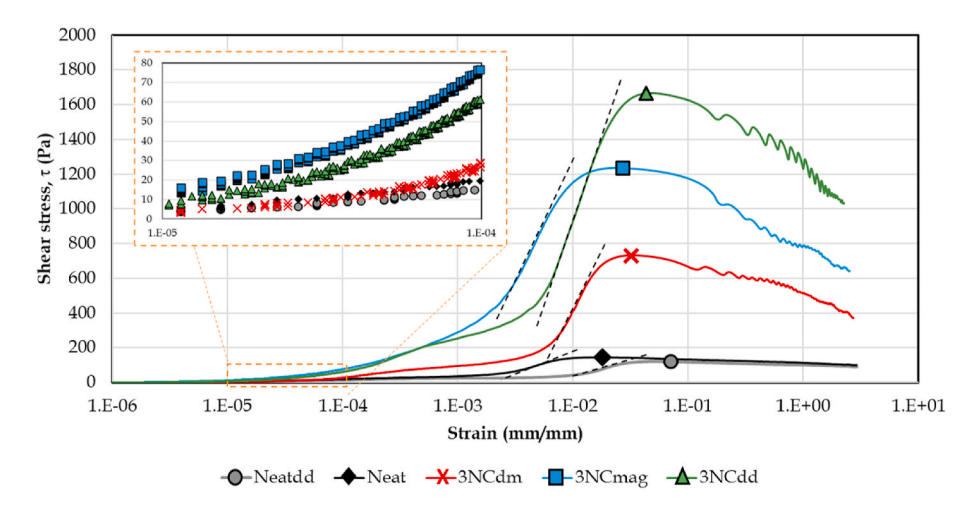


Fig. 13. Stress-strain curves of cement paste at 3 wt% NC dosage using dry mixing (dm), magnetic stirring (mag) and dry dispersion (dd) with linear regions representing strain levels where G'macro is measured.

higher sensitivity to properties that include soft interactions, i.e. static yield and G'<sub>macro</sub>, compared to only rigid interactions, i.e. SAOS. For example, the upper limit of increase in static yield stress for dd is 1500%

compared to 550% in storage modulus. There is also a significant shift in the increase magnitude between the corresponding macroscopic stress at strain values in the  $10^{-3}$ - $10^{-2}$  range compared to  $10^{-5}$  to  $10^{-4}$  (See

the small box in Fig. 13). These results indicate that NC has greater impact on colloidal interactions rather than rigid forces. We also see significant change in the NC efficiency with increasing dispersion energy. This relationship is discussed in more depth later on.

### 4.4. Rheology - Kerosene system

To further study colloidal interactions, we use dd NC-cement in kerosene solutions. This method of dispersion was used because NC are not dispersible in kerosene by using magnetic stirring and because dd is significantly more efficient than dm. Further, kerosene prevents hydration, eliminating the influence of any early hydrates and leaving only colloidal interactions. It is known that there are two main types of noncontact colloidal interaction existing in a cementitious system if we do not consider the steric hindrance induced by polymer additives: Van der Waals forces and electrostatic forces from adsorbed ions. By using kerosene as the suspending medium, we can diminish the influence of electrostatic force in cement paste. Kerosene is a nonpolar solvent, as opposed to water or isopropyl/ethyl alcohol, and hence we expect that electrostatic interactions are weak compared to aqueous phases and may be considered as negligible on the basis of solvation energy arguments [44]. We also looked at different NC contents up to 4.0 wt%, measuring both static yield and storage modulus, as shown in Fig. 14. The addition of NC showed insignificant effects on both static yield stress and storage modulus considering statistical significance. Because we observed significant changes in static yield stress in cement-water pastes modified with NC and none in the cement-kerosene pastes, we can deduce that the origins of colloidal interactions of NC in cement-based systems are mainly ionic bonds and electrostatic interactions due to dissolution. As a result, higher degree of dispersion would potentially increase the number of potential interactions. This in part explains why dd, which utilizes the highest dispersion energy, shows the highest static yield stress, followed by mag then dm.

# 4.5. Calorimetry - cement paste systems

In section 4.3, we discussed that the results of storage modulus suggest stronger rigid structure, either through linking of cements by early hydrates or the NC themselves. And the results of  $G_{\rm rigid}$  indicated NC dispersed by all methods led to an increase in rate of storage modulus evolution, although threshold levels were observed. To further characterize this effect and expand its relationship with hydration kinetics, we can analyze the results of isothermal calorimetry of dm, mag and dd shown in Figs. 15, 16 and 17, respectively. In Fig. 15, we identify 3 critical points: #1 is associated with surface reaction  $C_3S$  and measures the end of the dormant period (also called termination peak) and the

start of the acceleration period [34,38,45], #2 marks the main  $C_3S$  reaction indicating complete setting and the beginning of early hardening and strength development, and #3 marks the main  $C_3A$  reaction indicating ettringite formation, sulfate depletion and the end of the acceleration period [34,46]. Point #1 has been shown through isothermal calorimetry and cold field emission SEM to identify the shift from surface C–S–H nucleation to C–S–H growth and is mainly affected by change in surface area [38]. It should be noted that because NC are added as weight replacement of cement, pastes with higher NC content are more diluted. The dilution effect would cause a small backward time shift (moving to the right) in point #1 and small reduction in maximum heat of hydration in the acceleration peak.

NC have been suggested to have nucleation or seeding potential [14, 47,48], which would result in a forward time shift in point #1 with an increase in NC content. NC-cement pastes prepared with dm and dd showed an insignificant difference at 1 wt% and a forward shift (earlier) with increasing NC content up to 3.0 wt% for point #1. Cement pastes prepared via mag showed a forward shift in peak #1 irrespective of NC content, statistically speaking. These results only agree marginally with the relationship between nucleation potential and expected shift in point #1. Thus, either the resolution of the isothermal calorimetry test was not enough to capture this phenomenon, or nucleation potential cannot fully explain the origin of how NC is increasing modulus. To clarify the contribution of hydration versus nanoclay on structure will require further investigation on build-up kinetics and is out of the scope of the present paper. Nevertheless, all NC cement pastes, regardless of their method of dispersion, show higher peaks of heat of hydration at the acceleration period in agreement with other researchers [7,14,29]. This also agrees with the results of storage modulus evolution (Fig. 11).

#### 5. Discussion

Our results showed an increase in static yield stress at significantly higher levels than storage modulus, 1500% compared to 550%, respectively, which suggests that the contribution of soft ionic forces due to addition of NC are greater than rigid forces. Our prior discussion in the background and motivation further shows that the main driver of the soft colloidal forces are NC-NC interactions. Since our results show higher NC efficiency for dd, mag and then dm in static yield stress, dynamic viscosity, storage modulus and macroscopic elastic modulus, the state of NC dispersion must be critical to the number of NC-NC and NC-cement interactions. Dispersion of nanomaterials encompasses two main features: disentangling or breaking apart agglomerates and distributing nanomaterials uniformly within the medium. The prior can be characterized through imaging while the latter is examined through consistency and magnitude of measured behavior. Yazdanbakhsh and Z.

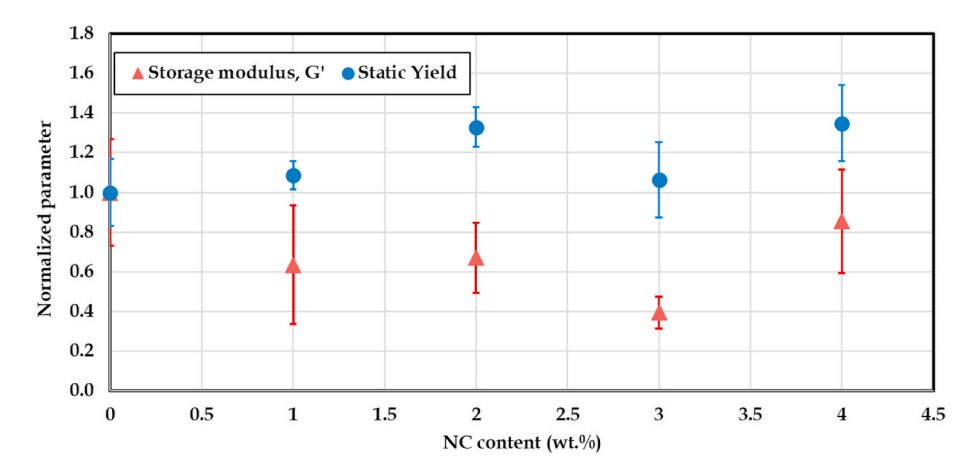


Fig. 14. Normalized static yield stress and storage modulus (G') as a function of NC content using dd cement and kerosene, where the reference neat (Neatddkero) has static yield of 656 Pa and storage modulus of  $1.4 \times 10^6$  Pa.

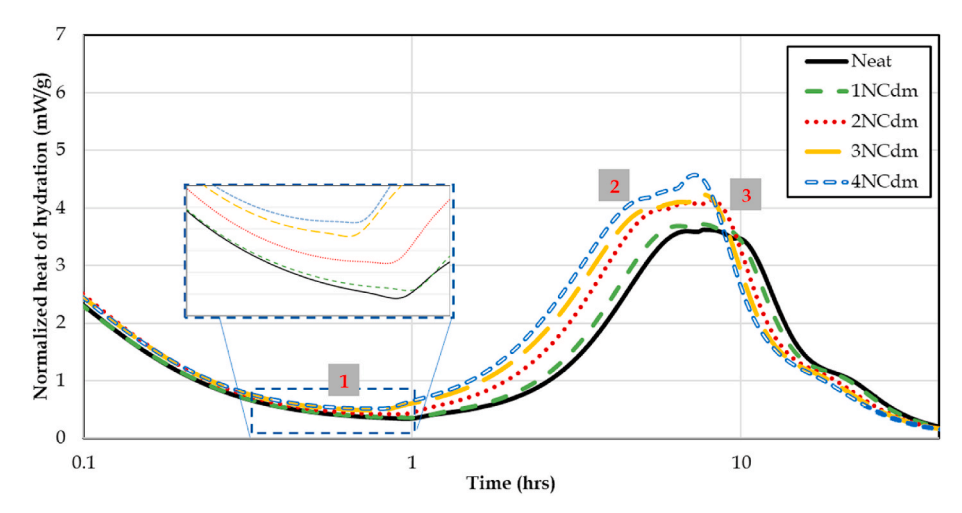


Fig. 15. Heat of hydration kinetics curves of NC-cement paste prepared through dry mixing (dm).

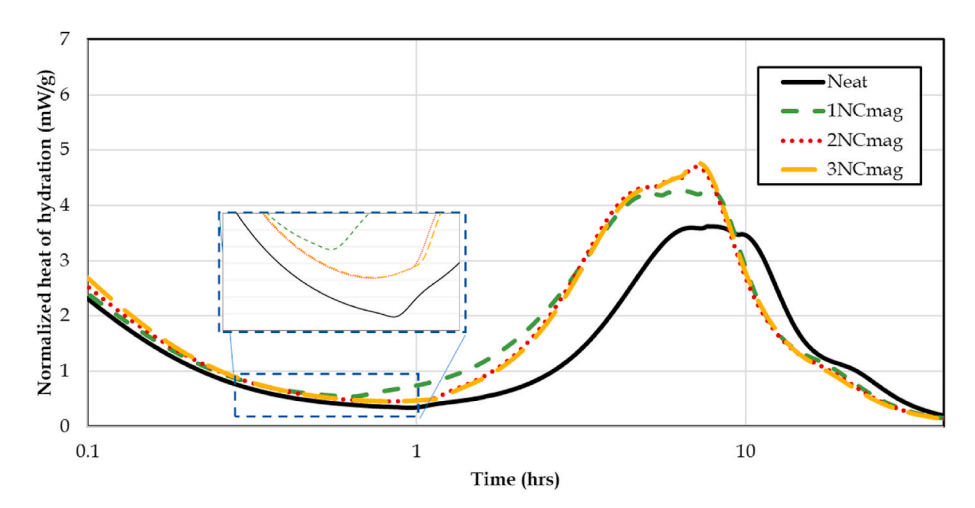


Fig. 16. Heat of hydration kinetics curves of NC-cement paste prepared through magnetic stirring (mag).

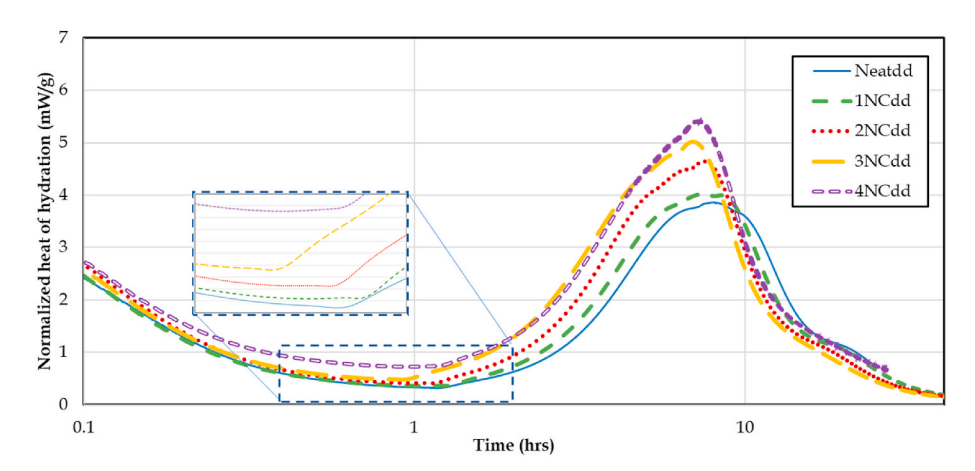


Fig. 17. Heat of hydration kinetics curves of NC-cement paste prepared through dry mixing (dd).

Garsley concluded that uniform dispersion in cement composites requires deagglomerated cement particles [16]. Because cement most often is in an agglomerated state [3], uniform solution dispersion of nanomaterials cannot produce uniform dispersion in cement composites. Of the three dispersion methods investigated, dd is the only method where both NC and cement are deagglomerated at the same time due to sonication of both in ethanol. Therefore, we suggest that of the three

investigated dispersion methods, dd has the most uniform dispersion with the highest number of deagglomerated or individual NC needles. Since cement pastes prepared via mag and dm utilize similar mixing energy to distribute NC within the cement matrix, the investment of energy to disentangle and deagglomerate NC is critical to maximize NC efficiency on the rheological response of cement paste.

3DCP remains in its initial stages of development, which includes

significant developments in rheological models and additives, printers, extruders, pumps, printing properties and mechanical/structural performance. Similar to current construction methods, this technology should be applicable in pre-cast facilities as well as on site. The additive system used to achieve the rheological demand should be efficient, scalable, low maintenance and versatile. Currently, significant delays can be expected due to printing errors, weather or machinery related delays. For example, Diggs-McGee et al. showed that for the construction time of 5 days, the actual printing time is 14 h and the elapsed printing-active time is 31 h [49]. Nanomodified cement through dd offers a simple method of using NC cement on site and offers an extended shelf life, compared to solution dispersions that may segregate over time. This method also shows higher efficiency in increasing the static yield stress by up to 1500% with a maximum increase in viscosity of 90%. The stiffness of the resulting layers characterized by G'macro is also significantly higher than other methods, a key factor in buildability and shape stability [1].

The static yield stress can be directly applied to the maximum layer height possible according to Roussel:  $\tau_v \ge gh_0$ , where  $\tau_v$  is the static yield stress,  $\rho$  is the density, g is the gravity and  $h_0$  is the individual layer height [1]. Fig. 18 shows the corresponding maximum initial layer height possible where dd can reach initial layer heights of 81.5 mm at 4 wt% content. Regardless of the print height however, structural stability remains critical in 3DCP applications. In fact, the structural stability is significantly impacted by the print geometry and specifically the print slenderness ratio (H/ $\delta$ ). Roussel has also estimated structural stability by considering the effect of buckling on a one linear meter long, unbraced wall through:  $E > 3gH^3/2\delta^2$  where E is the elastic modulus (referred to in this work as  $G'_{macro}),$  H is the total print height and  $\delta$  is the layer width [1]. Prints where geometry allows for internal structural bracing can have higher possible print height or lower critical elastic modulus. This relationship is then very useful in approximating the structural stability of unbraced segments within a print. In Fig. 19 we show this relationship for some of the highest contents of NC examined for each dispersion method. It is important to note that the E value used here was measured shortly after an extended pre-shear (in the protocol in Fig. 3, the low strain rate step) so the print height, H, is that of the freshly deposited layer, before the development of green strength as the material rests. But this early E is important as it will set the initial condition for layer stability. As suggested by our storage modulus evolution (Fig. 11), there is a continuous growth of E due to increased nucleation that further increases the layer stiffness and stability. As discussed with respect to the macroscopic elastic modulus (Fig. 12), higher content of NC increases the elastic modulus and consequently shape stability. In fact, only cement with NC would produce structurally stable layer depositions with a slenderness ratio of 10. 4NCdd offers the highest shape stability despite the fact that the reference cement for dd is significantly less stiff than the unprocessed Neat cement. This preliminary analysis shows that NC's impact on rheology translates to significant improvements in printing properties, specifically enhanced buildability and shape stability, and these improvements scale with NC content and energy utilized in dispersion.

#### 6. Conclusion

We examined various dispersion methods for NC (dry mixing, magnetic stirring in solution, and dry dispersion) and tested their impact on rheological and hydration behavior of cement pastes. Dry dispersion is a new dispersion method that successfully coats cement grains with NC needles. NC cement paste tests included rheological measurements (i.e. static yield stress, viscosity, and small amplitude oscillation shear), SEM imaging, and isothermal calorimetry. Our results show that there is a significantly higher increase in static yield stress, up to 1500%. compared to that of storage modulus, limited to 550%, with the addition of NCdd up to 4%, and no increase in either of these parameters in the kerosene NC-cement systems. As a result, we suggest that soft colloidal interactions due to adsorbed ions play a more significant role in increasing the static yield stress than rigid interactions or Van der Waals forces. Within these soft adsorbed ionic forces, we discussed how NCcement, NC-NC and cement-cement interactions are affected by the addition of NC. We also examined the effect of NC dispersion on rheology, and we discussed NC potential for 3DCP. Our results show:

- Static yield stress and storage modulus increased from reference cement paste by up to 1500% and 550%, respectively. The increase was proportional to NC content up to 4%wt with minimal increase in viscosity by up to 90%.
- The efficiency of NC in altering the rheological response of cement paste was higher for methods with higher dispersion energy: dry dispersion, magnetic stirring followed by dry mixing.
- Heat of hydration during the acceleration period increased with NC content and dispersion energy.
- It is possible to significantly reduce the required NC dosage for 3DCP by utilizing dry dispersion, which is a method that has no dispersion decay as it disperses on solid rather than in solution.
- The higher NC efficiency in static yield stress compared to storage modulus observed in our results indicate that NC-NC soft interactions (specifically from adsorbed ions per our kerosene system investigation) are the main driver of static yield stress structuration.

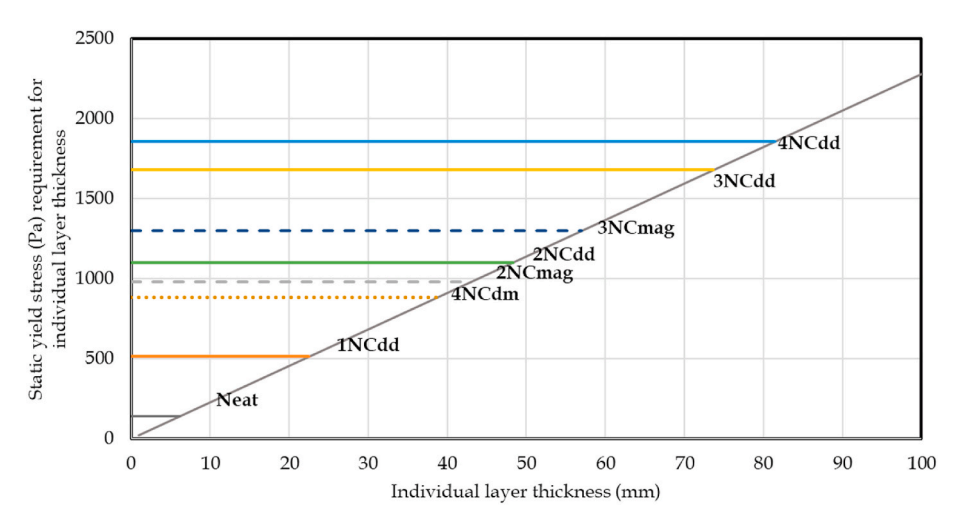


Fig. 18. Static yield stress requirement for individual layer thickness based on N. Roussel's τ y≥ρgh\_0 [1] assuming density of 2.32 g/cm<sup>3</sup>.

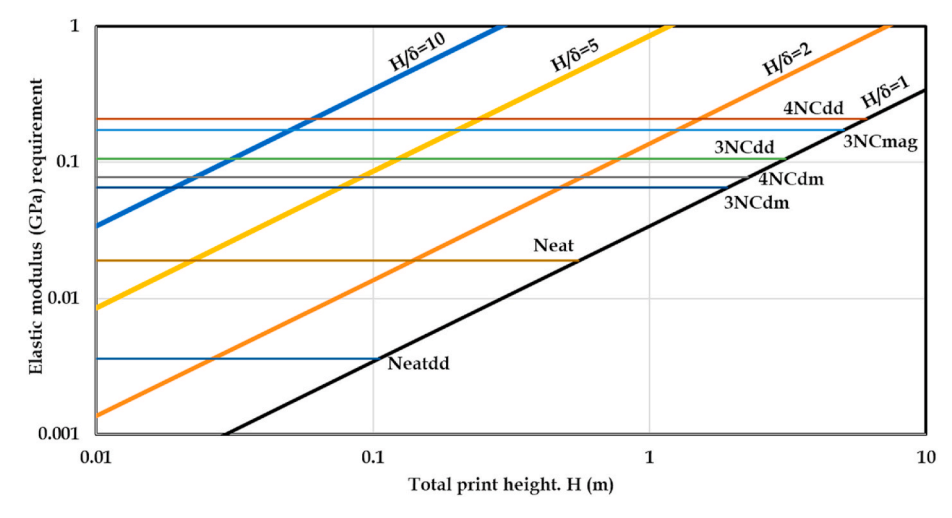


Fig. 19. Print structural stability measured by the relationship between the elastic modulus and total print height given different print slenderness ratio ( $H/\delta$ ) assuming density of 2.32 g/cm<sup>3</sup>.

- NC increases C–S–H growth and potentially surface-based C–S–H nucleation, which corresponds to increased rigidification and stiffness.
- The effect of NC on static yield stress, storage modulus and its storage modulus evolution can lead to high buildability and shape stability for 3DCP.

# Declaration of competing interest

The authors declare that they have no known competing financial interests or personal relationships that could have appeared to influence the work reported in this paper.

# Acknowledgements

The authors would like to acknowledge the National Science Foundation (Award #1653419) for financial support, and technical support by the staff of Columbia University's Carleton Laboratory.

#### References

- N. Roussel, Rheological requirements for printable concretes, Cement Concr. Res. 112 (2018) 76–85, https://doi.org/10.1016/j.cemconres.2018.04.005. ISSN 2020. 2021.
- [2] N. Roussel, G. Ovarlez, S. Garrault, C. Brumaud, The origins of thixotropy of fresh cement pastes, Cement Concr. Res. 42 (1) (2012) 148–157, https://doi.org/ 10.1016/j.cemconres.2011.09.004. ISSN 0008–8846.
- [3] R.J. Flatt, Dispersion forces in cement suspensions, Cement Concr. Res. 34 (3) (2004) 399–408, https://doi.org/10.1016/j.cemconres.2003.08.019. ISSN 0008-8846
- [4] R.J. Flatt, P. Bowen, Electrostatic repulsion between particles in cement suspensions: domain of validity of linearized Poisson–Boltzmann equation for nonideal electrolytes, Cement Concr. Res. 33 (6) (2003) 781–791, https://doi.org/ 10.1016/S0008-8846(02)01059-1. ISSN 0008-8846.
- [5] J. Kruger, S. Zeranka, G. Zijl, 3D concrete printing: a lower bound analytical model for buildability performance quantification, Autom. ConStruct. 106 (2019) 102904, https://doi.org/10.1016/j.autcon.2019.102904. ISSN 0926-5805.
- [6] R. Jayathilakage, P. Rajeev, J.G. Sanjayan, Yield stress criteria to assess the buildability of 3D concrete printing, Construct. Build. Mater. 240 (2020) 117989, https://doi.org/10.1016/j.conbuildmat.2019.117989. ISSN 0950-0618.
- [7] A.V. Rahul, M. Santhanam, H. Meena, Z. Ghani, 3D printable concrete: mixture design and test methods, Cement Concr. Compos. 97 (2019) 13–23. ISSN 0958–9465.
- [8] A. Kazemian, X. Yuan, E. Cochran, B. Khoshnevis, Cementitious materials for construction-scale 3D printing: Laboratory testing of fresh printing mixture, Construct. Build. Mater. 145 (2017) 639–647. ISSN 0950–0618.
- [9] D.G. Soltan, V.C. Li, A self-reinforced cementitious composite for building-scale 3D printing, Cement Concr. Compos. 90 (2018) 1–13. ISSN 0958–9465.
- [10] O.A. Mendoza Reales, P. Duda, E.C.C.M. Silva, M.D.M. Paiva, R.D.T. Filho, Nanosilica particles as structural buildup agents for 3D printing with Portland cement pastes, Construct. Build. Mater. 219 (2019) 91–100, https://doi.org/ 10.1016/j.conbuildmat.2019.05.174. ISSN 0950–0618.

- [11] B. Panda, M.J. Tan, Experimental study on mix proportion and fresh properties of fly ash based geopolymer for 3D concrete printing, Ceram. Int. 44 (9) (2018) 10258–10265. ISSN 0272–8842.
- [12] B. Panda, S.C. Paul, L.J. Hui, Y.W.D. Tay, M.J. Tan, Additive manufacturing of geopolymer for sustainable built environment, J. Clean. Prod. 167 (2017) 281–288. 0959–6526.
- [13] M. Kaszyńska, M. Hoffmann, S. Skibicki, A. Zieliński, M. Techman, N. Olczyk, T. Wróblewski, Evaluation of suitability for 3D printing of high performance concretes, MATEC web of conferences 163 (2018) 1002, https://doi.org/10.1051/ matecconf/201816301002, 2261–236X.
- [14] Y. Zhang, Y. Zhang, G. Liu, Y. Yang, M. Wu, B. Pang, Fresh properties of a novel 3D printing concrete ink, Construct. Build. Mater. 174 (2018) 263–271. ISSN 0950–0618.
- [15] B. Panda, S. Ruan, C. Unluer, M.J. Tan, Improving the 3D printability of high volume fly ash mixtures via the use of nano attapulgite clay, Compos. B Eng. 165 (2019) 75–83. ISSN 1359–8368.
- [16] A. Yazdanbakhsh, Z. Grasley, The theoretical maximum achievable dispersion of nanoinclusions in cement paste, Cement Concr. Res. 42 (6) (2012) 798–804.
- [17] T. Wangler, E. Lloret, L. Reiter, N. Hack, F. Gramazio, M. Kohler, M. Bernhard, B. Dillenburger, J. Buchli, N. Roussel, R. Flatt, Digital concrete: opportunities and challenges, RILEM Technical Letters 1 (2016) 67–75, https://doi.org/10.21809/ rilemtechlett.2016.16.
- [18] D.P. Bentz, S.Z. Jones, I.R. Bentz, M.A. Peltz, Towards the formulation of robust and sustainable cementitious binders for 3-D additive construction by extrusion, Construct. Build. Mater. 175 (2018) 215–224. ISSN 0950-0618.
- [19] B. Panda, J.H. Lim, M.J. Tan, Mechanical properties and deformation behaviour of early age concrete in the context of digital construction, Compos. B Eng. 165 (2019) 563–571. ISSN 1359–8368.
- [20] D. Jiao, C. Shi, Q. Yuan, X. An, Y. Liu, H. Li, Effect of constituents on rheological properties of fresh concrete-A review, Cement Concr. Compos. 83 (2017) 146–159, https://doi.org/10.1016/j.cemconcomp.2017.07.016. ISSN 0958–9465.
- [21] Y. Qian, S. Ma, S. Kawashima, G.D. Schutter, Rheological characterization of the viscoelastic solid-like properties of fresh cement pastes with nanoclay addition, Theor. Appl. Fract. Mech. 103 (2019) 102262, https://doi.org/10.1016/j. cemconres.2016.09.005. ISSN 0167-8442.
- [22] Y. Qian, S. Kawashima, Use of creep recovery protocol to measure static yield stress and structural rebuilding of fresh cement pastes, Cement Concr. Res. 90 (2016) 73, 0008-8846.
- [23] S. Ma, Y. Qian, S. Kawashima, Experimental and modeling study on the non-linear structural build-up of fresh cement pastes incorporating viscosity modifying admixtures, Cement Concr. Res. 108 (2018) 1, https://doi.org/10.1016/j. cemconres.2018.02.022, 0008-8846.
- [24] I. Dejaeghere, M. Sonebi, G. De Schutter, Influence of nano-clay on rheology, fresh properties, heat of hydration and strength of cement-based mortars, Construct. Build. Mater. 222 (2019) 73–85. ISSN 0950–0618.
- [25] Y. Liu, J. Han, M. Li, P. Yan, Effect of a nanoscale viscosity modifier on rheological properties of cement pastes and mechanical properties of mortars, Construct. Build. Mater. 190 (2018) 255–264. ISSN 0950–0618.
- [26] ActiveMinerals International, LLC. What is Acti-Gel® 208 and the science behind Acti-Gel® 208.
- 27] Y. Qian, G. De Schutter, Enhancing thixotropy of fresh cement pastes with nanoclay in presence of polycarboxylate ether superplasticizer (PCE), Cement Concr. Res. 111 (2018) 15–22. ISSN 0008–8846.
- [28] N.A. Tregger, M.E. Pakula, S.P. Shah, Influence of clays on the rheology of cement pastes, Cement Concr. Res. 40 (3) (2010) 384–391. ISSN 0008–8846.
- [29] Z. Quanji, G.R. Lomboy, K. Wang, Influence of nano-sized highly purified magnesium alumino silicate clay on thixotropic behavior of fresh cement pastes, Construct. Build. Mater. 69 (2014) 295–300. ISSN 0950–0618.

- [30] T. Chang, J. Shih, K. Yang, T. Hsiao, Material properties of portland cement paste with nano-montmorillonite, J. Mater. Sci. 42 (17) (2007) 7478. ISSN: 0022–2461.
- [31] S. Parveen, S. Rana, R. Fangueiro, A review on nanomaterial dispersion, microstructure, and mechanical properties of carbon nanotube and nanofiber reinforced cementitious composites, J. Nanomater. 19 (2013), https://doi.org/ 10.1155/2013/710175.
- [32] S. Pradhan, J. Hedberg, E. Blomberg, S. Wold, I.O. Wallinder, Effect of sonication on particle dispersion, administered dose and metal release of non-functionalized, non-inert metal nanoparticles, J. Nanoparticle Res.: an interdisciplinary forum for nanoscale science and technology 18 (9) (2016) 1, https://doi.org/10.1007/ s11051-016-3597-5, 1572-896X.
- [33] Z. Guo-Dong, J.D. Kuntz, J. Wan, A.K. Mukherjee, Single-wall carbon nanotubes as attractive toughening agents in alumina-based nanocomposites, Nat. Mater. 2 (1) (2002) 38, https://doi.org/10.1038/nmat793. ISSN: 1476-4660.
- [34] J.M. Makar, G.W. Chan, Growth of cement hydration products on single walled carbon nanotubes, J. Am. Ceram. Soc. 92 (6) (2009) 1303, https://doi.org/ 10.1111/j.1551-2916.2009.03055.x. ISSN: 0002-7820.
- [35] J.M. Makar, J. Margeson, J. Luh, Carbon nanotube/cement composites-early results and potential applications, Construction Materials, in: Proceedings of ConMat'05 and Mindess Symposium, Canada, Vancouver, 2005, p. 32.
- [36] J. Hogancamp, Z. Grasley, The use of microfine cement to enhance the efficacy of carbon nanofibers with respect to drying shrinkage crack resistance of portland cement mortars, Cement Concr. Compos. 83 (2017) 405–414. ISSN 0958–9465.
- [37] V.V. Rocha, P. Ludvig, A.C.C. Trindade, F. de Andrade Silva, The influence of carbon nanotubes on the fracture energy, flexural and tensile behavior of cement based composites, Construct. Build. Mater. 209 (2019) 1–8. ISSN 0950–0618, [38] J. M. Makar, G.W. End of the Induction Period in Ordinary Portland Cement as Examined by High-Resolution Scanning Electron Microscopy. Journal of the American Ceramic Society, 4/2008, ISSN: 0002-7820, Volume 91, Issue 4, p. 1292.
- [38] E. Sakai, M. Daimon, Mechanisms of superplastification, in: J. Skalny, S. Mindess (Eds.), Materials Science of Concrete vol. IV, Amercian Ceramic Society, Westerville, OH, 1995, pp. 91–111.

- [39] S. Mantellato, M. Palacios, R.J. Flatt, Relating early hydration, specific surface and flow loss of cement pastes, Mater. Struct. 52 (5) (2019), https://doi.org/10.1617/ s11527-018-1304-y.
- [40] Y. Liu, J. Han, M. Li, P. Yan, Effect of a nanoscale viscosity modifier on rheological properties of cement pastes and mechanical properties of mortars, Construct. Build. Mater. 190 (2018) 255–264, https://doi.org/10.1016/j.conbuildmat.2018.09.110. ISSN 0950-0618.
- [41] R.D. Ferron, S. Shah, E. Fuente, C. Negro, Aggregation and breakage kinetics of fresh cement paste, Cement Concr. Res. 50 (2013) 1–10, https://doi.org/10.1016/ j.cemconres.2013.03.002. ISSN 0008–8846.
- [42] N.A. Tregger, M.E. Pakula, Surendra P. Shah, Influence of clays on the rheology of cement pastes, Cement Concr. Res. 40 (3) (2010) 384–391, https://doi.org/ 10.1016/j.cemconres.2009.11.001. ISSN 0008–8846.
- [43] G. Kokot, M.I. Bespalova, M. Krishnan, Measured electrical charge of SiO2 in polar and nonpolar media, J. Chem. Phys. 145 (2016) 194701, https://doi.org/10.1063/ 1.4967401
- [44] J.M. Makar, G.W. Chan, K.Y. Esseghaier, A peak in the hydration reaction at the end of the cement induction period, J. Mater. Sci. 42 (4) (2007) 1388. ISSN: 0022–2461.
- [45] S. Mindness, J.F. Yong, D. Darwin, Concrete, Prentice Hall, Upper Saddle River (New Jersey, 2003.
- [46] N. Hamed, M.S. El-Feky, M. Kohail, E.A.R. Nasr, Effect of nano-clay deagglomeration on mechanical properties of concrete, Construct. Build. Mater. 205 (2019) 245, 0950-0618.
- [47] H. Lindgreen, M. Geiker, H. Krøyer, N. Springer, J. Skibsted, Microstructure engineering of Portland cement pastes and mortars through addition of ultrafine layer silicates, Cement Concr. Compos. 30 (8) (2008) 686, 0958-9465.
- [48] B.N. Diggs-McGee, E.L. Kreiger, M.A. Kreiger, M.P. Case, Print time vs. elapsed time: a temporal analysis of a continuous printing operation for additive constructed concrete, Additive Manufacturing 28 (2019) 205–214, 2214–8604.